GEOLOGICAL SURVEY OF CANADA
OPEN FILE 7856

Targeted Geoscience Initiative 4: Canadian Nickel-Copper-Platinum Group Elements-Chromium Ore Systems — Fertility, Pathfinders, New and Revised Models

A geological, petrological, and geochronological study of the Grey Gabbro unit of the Podolsky Cu-(Ni)-PGE deposit, Sudbury, Ontario, with a focus on the alteration related to the formation of sharp-walled chalcopyrite veins

Daniel J. Kontak[1], Linette M. MacInnis[1], Doreen E. Ames[2], Nicole M. Rayner[2], and Nancy Joyce[2]

[1]Laurentian University, Sudbury, Ontario
[2]Geological Survey of Canada, Ottawa, Ontario

2015

Recommended citation

Kontak, D.J., MacInnis, L.M., Ames, D.E., Rayner, N.M., and Joyce, N., 2015. A geological, petrological, and geochronological study of the Grey Gabbro unit of the Podolsky Cu-(Ni)-PGE deposit, Sudbury, Ontario, with a focus on the alteration related to the formation of sharp-walled chalcopyrite veins, *In:* Targeted Geoscience Initiative 4: Canadian Nickel-Copper-Platinum Group Elements-Chromium Ore Systems — Fertility, Pathfinders, New and Revised Models, (ed.) D.E. Ames and M.G. Houlé; Geological Survey of Canada, Open File 7856, p. 287–301.

Publications in this series have not been edited; they are released as submitted by the author.

Contribution to the Geological Survey of Canada's Targeted Geoscience Initiative 4 (TGI-4) Program (2010–2015)

TABLE OF CONTENTS

A geological, petrological, and geochronological study of the Grey Gabbro unit of the Podolsky Cu-(Ni)-PGE deposit, Sudbury, Ontario, with a focus on the alteration related to the formation of sharp-walled chalcopyrite veins

Daniel J. Kontak[1]*, Linette M. MacInnis[1], Doreen E. Ames[2], Nicole M. Rayner[2], and Nancy Joyce[2]

[1]Mineral Exploration Research Centre, Department of Earth Sciences, Laurentian University, 935 Ramsey Lake Road, Sudbury, Ontario P3E 2C6
[2]Geological Survey of Canada, 601 Booth Street, Ottawa, Ontario K1A 0E8
*Corresponding author's e-mail: dkontak@laurentian.ca

ABSTRACT

An integrated geological, petrological, and geochronological study of the Grey Gabbro (GG) unit of the Podolsky Cu-(Ni)-PGE deposit, which is located in a radial dyke of the 1850 Ma Sudbury Igneous Complex (SIC), indicates it is a dislodged fragment of alkalic gabbroic basement rock with a minimum age of ca. 2714 Ma (U-Pb zircon). Petrographic textures in the GG record both the impact event (e.g. planar deformation features in zircon) and subsequent thermal overprinting from the cooling SIC melt sheet; U-Pb dating of epitaxial zircon overgrowths yielded concordant dates at ca. 1850 Ma. Petrological study of the GG adjacent to sharp-wall chalcopyrite veins provides a number of insights into the origin of mineralization in the high-sulphide Cu-PGE Podolsky deposit. 1) Actinolite fibres (<1–2 cm) occur both at vein margins and within the sulphide veins, indicating that they are synchronous with or pre-date vein injection. 2) Intense alteration with the formation of actinolite-epidote-quartz-chalcopyrite-magnetite assemblages is restricted in the GG to within <1–2 cm of vein margins. The same alteration assemblage does occur <20–30 cm into the GG but as micro-clots (<1 mm) and post-dates the thermal effects of the cooling SIC; hence, this provides a time frame for massive chalcopyrite vein formation. (3) At distances of >1 m from the sulphide veins, geochemical modification from fluid:rock interaction is minimal in the GG, with Cu the only distal indicator of mineralization (i.e. 100s ppm Cu). 4) Isotopic data (Sr, O, S) indicate that S in the Podolsky deposit is similar to that of the Whistle contact Ni-Cu deposit and is sourced from the melt sheet ($\delta^{34}S_{cpy}$ = 4.3‰). These observations indicate that alteration within the GG is the result of the equilibration of high-temperature magmatic-derived fluids with the GG and that the GG is part of the pre-impact history of the area. Intense hydrothermal alteration in the GG occurs only adjacent (<10s cm) to the sharp-walled sulphide veins and thus does not provide a significant vector for exploration.

INTRODUCTION

The Podolsky Cu-(Ni)-PGE deposit, located in Norman township ~35 km north-northeast of Sudbury, is hosted by the Whistle-Parkin radial offset dyke that radiates outwards from an embayment structure in the Paleoproterozoic 1850 Ma (Krogh et al., 1984) Sudbury Igneous Complex (SIC; Fig. 1a,b). The Podolsky 2000 deposit (Fig. 1b) was an underground mine that produced ~1.5 M tonnes of 4.29% Cu, 0.38% Ni, 0.051 oz/t Pt, 0.054 oz/t Pd, and 0.024 oz/t Au, between 2007 and 2011 (Courtesy of KGHM International Ltd.). This deposit is a hybrid style deposit that displays aspects of both "sharp-walled" and "low-sulphide" style mineralization in the Sudbury Structure (Farrow et al., 2005). The 2000 deposit is situated ~650 m below the formerly producing Ni-Cu-Co Whistle deposit, which is located at the basal contact of the SIC and the radial Whistle-Parkin offset structure (Fig. 1b,c). This offset, which is host to the Podolsky 2000 deposit, is a northeast-trending structure and is atypical compared to most radial offset structures, which are generally composed of quartz diorite material. Instead, this offset dyke is dominated by metabreccia rock (i.e. metamorphosed breccia rock) that contains small bodies of quartz diorite rock, inclusion-bearing quartz diorite, and pods of other intrusive phases that vary in size (i.e. <1 cm to 10s of m; Carter et al., 2009). One such pod in this offset dyke is a large fragment of gabbroic rock, which has been referred to informally as the grey gabbro (GG), that hosts part of

Kontak, D.J., MacInnis, L.M., Ames, D.E., Rayner, N.M., and Joyce, N., 2015. A geological, petrological, and geochronological study of the Grey Gabbro unit of the Podolsky Cu-(Ni)-PGE deposit, Sudbury, Ontario, with a focus on alteration related to formation of sharp-walled chalcopyrite veins, *In:* Targeted Geoscience Initiative 4: Canadian Nickel-Copper-Platinum Group Elements-Chromium Ore Systems — Fertility, Pathfinders, New and Revised Models, (ed.) D.E. Ames and M.G. Houlé; Geological Survey of Canada, Open File 7856, p. 287–301.

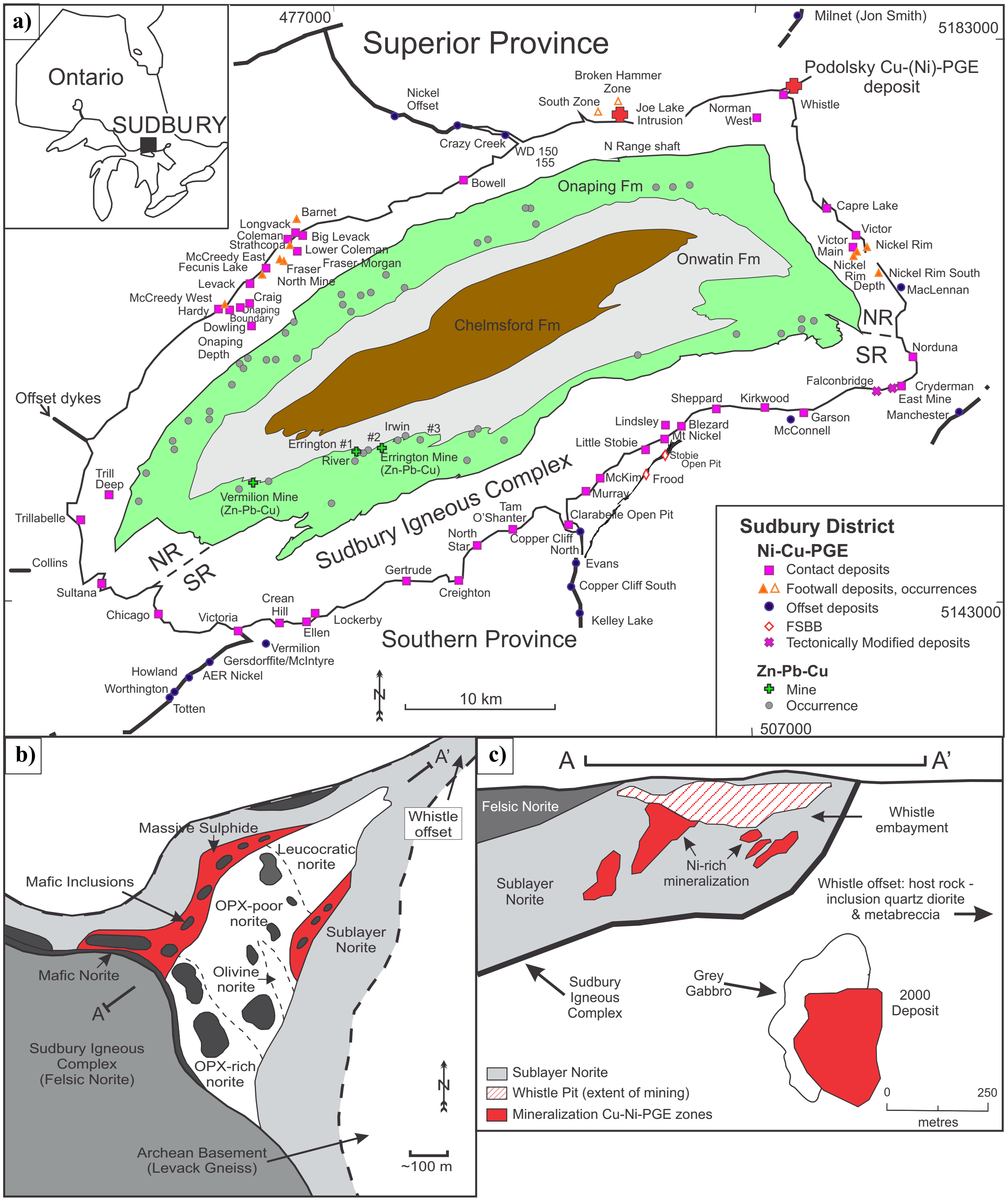

Figure. 1. a) Simplified geological map of the Sudbury Structure showing the footwall rocks, the Sudbury Igneous Complex (SIC) and related offset and concentric dyke rocks, and basin-fill material, as well as the location of the different types of sulphide deposits (i.e. contact, offset, footwall). Note the location of the Podolsky deposit and Joe Lake gabbro, both in the north part of the map area (red filled circles), which are referred to in the text. The figure is modified from Ames and Farrow (2007). **b)** A schematic plan view of the Whistle embayment structure of the SIC in relation to the Whistle-Parkin offset (modified from Lightfoot et al., 1997). The map shows the relationship between the main rock types of the SIC along with the beginning of the NE-trending Whistle-Parkin offset. Note the presence of SIC units, which include the inclusion-rich sublayer norite that hosted the Ni-rich contact-style mineralization mined from the Whistle Pit by INCO. **c)** A northeast long section (line A and A' in Fig. 1b) of the Whistle embayment that shows, from top down, felsic norite, sublayer norite, Ni-rich mineralization, Whistle-Parkin offset, the Grey Gabbro (GG) unit and the 2000 deposit. The study area was located in the GG fragment which hosts a series of sharp-walled chalcopyrite veins from the 2000 deposit. Figure has been modified from Farrow et al. (2005).

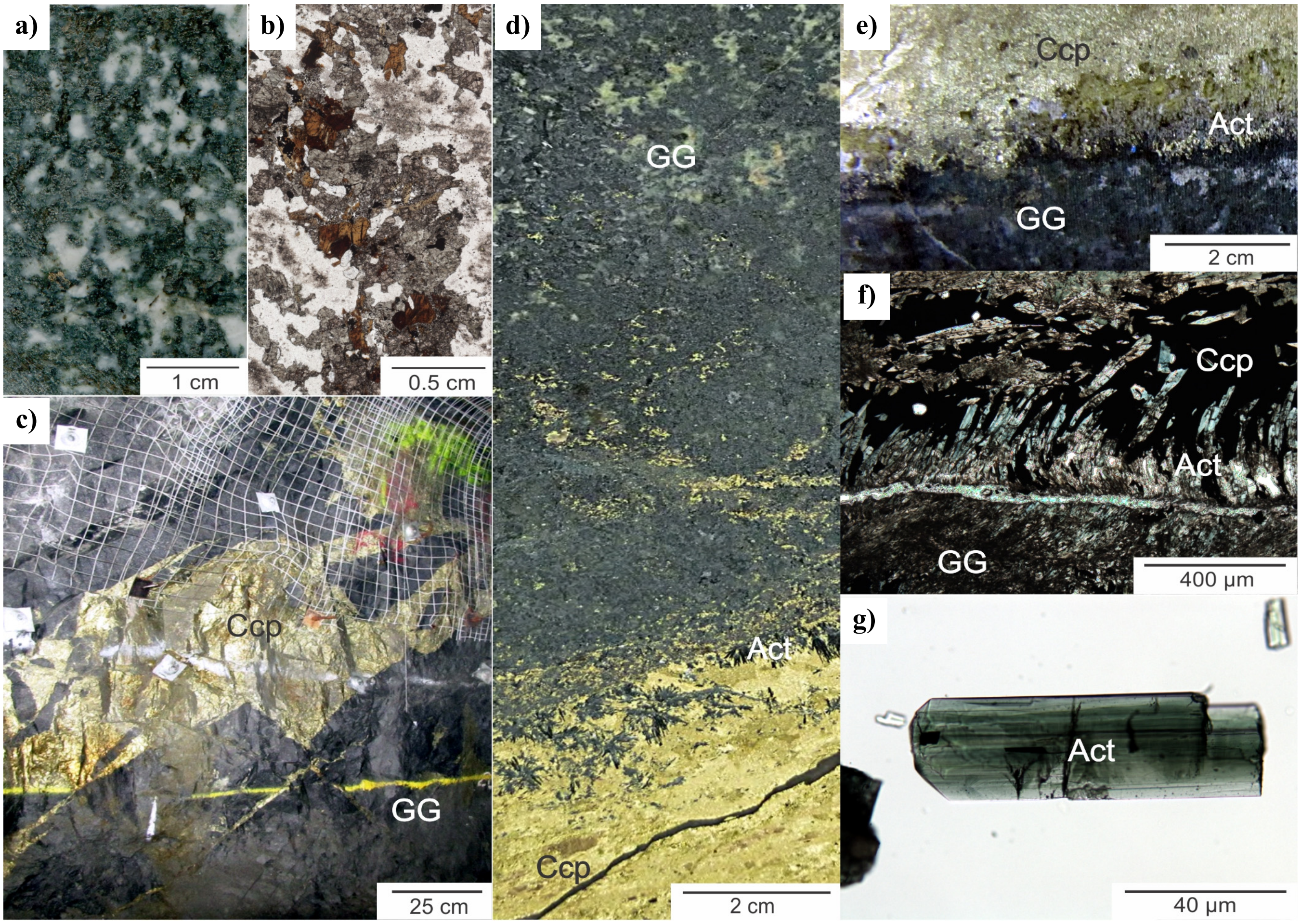

Figure. 2. Images of the Grey Gabbro (GG) unit and sharp-walled sulphide veins. **a)** Scanned rock slab of sample LM-P-007 showing the texture typical of the GG unit with mafic (i.e. pyroxene, amphibole, biotite) and felsic (i.e. plagioclase) domains. **b)** Thin section scan of sample LM-P-007 (in plane polarized light) showing the typical gabbroic-like texture, but note the unusual scalloped outlines of the plagioclase against the mafic domains and the dusty cores of the plagioclase due to alteration. The brown phase is biotite. **c)** Underground photo (1925 level) of a sharp-walled chalcopyrite vein cutting GG. **d)** Cut slab of sample LM-P-060 collected from the 1700 level. The sample shows, from top to bottom, the GG, intensely altered GG (actinolite-epidote), actinolite grains or fibres (Act) and massive chalcopyrite (Ccp) that entrains the actinolite grains. **e)** The GG in contact with a chalcopyrite sharp-walled vein with actinolite along the contact, as seen in drillhole FNX40272. **f)** Thin section photomicrograph (in plane polarized light) of sample LM-P-060 showing rotated actinolite fibres along the contact of a chalcopyrite vein. **g)** A grain of actinolite from a prepared mineral separate from sample LM-P-060 (see Fig. 2d) that was used for $^{40}Ar/^{39}Ar$ dating and isotope analyses (O, Sr).

the "sharp-walled" vein systems of the Podolsky 2000 deposit.

This paper summarizes the results of a graduate thesis project by the second author (L. MacInnis, M.Sc. thesis, in prep.) that documents the nature and extent of alteration in the GG unit (Figs. 2a,b, 3a,b), both proximal and distal to its contained footwall-style mineralization (Fig. 2c). The GG unit is, as noted above, a large (230 m by 270 m) fragment that occurs in the Whistle offset dyke, which hosts thick (<1 m) sharp-walled veins of massive chalcopyrite, many of which contain narrow (i.e. cm-scale) epidote-actinolite-magnetite-bearing alteration halos (Fig. 2d-f). More specifically, the focus of the study was to characterize the mineralogy and geochemistry of the alteration specific to the sharp-walled vein mineralization to further our understanding of footwall-styled ore systems and to see if such data may provide criteria for vectoring towards mineralization in other footwall environments of the SIC. The massive and homogenous nature of the GG unit, combined with underground access to it and the sharp-walled veins in addition to the availability of historic drill core, made this site ideal for such a project. The study was broken into two parts in order to achieve its objectives:

- Characterize the mineralogy and geochemistry of the least altered host rock (i.e. GG) to the mineralization, as this formed the basis for the subsequent alteration study;
- Assess the nature and origin of the alteration asso-

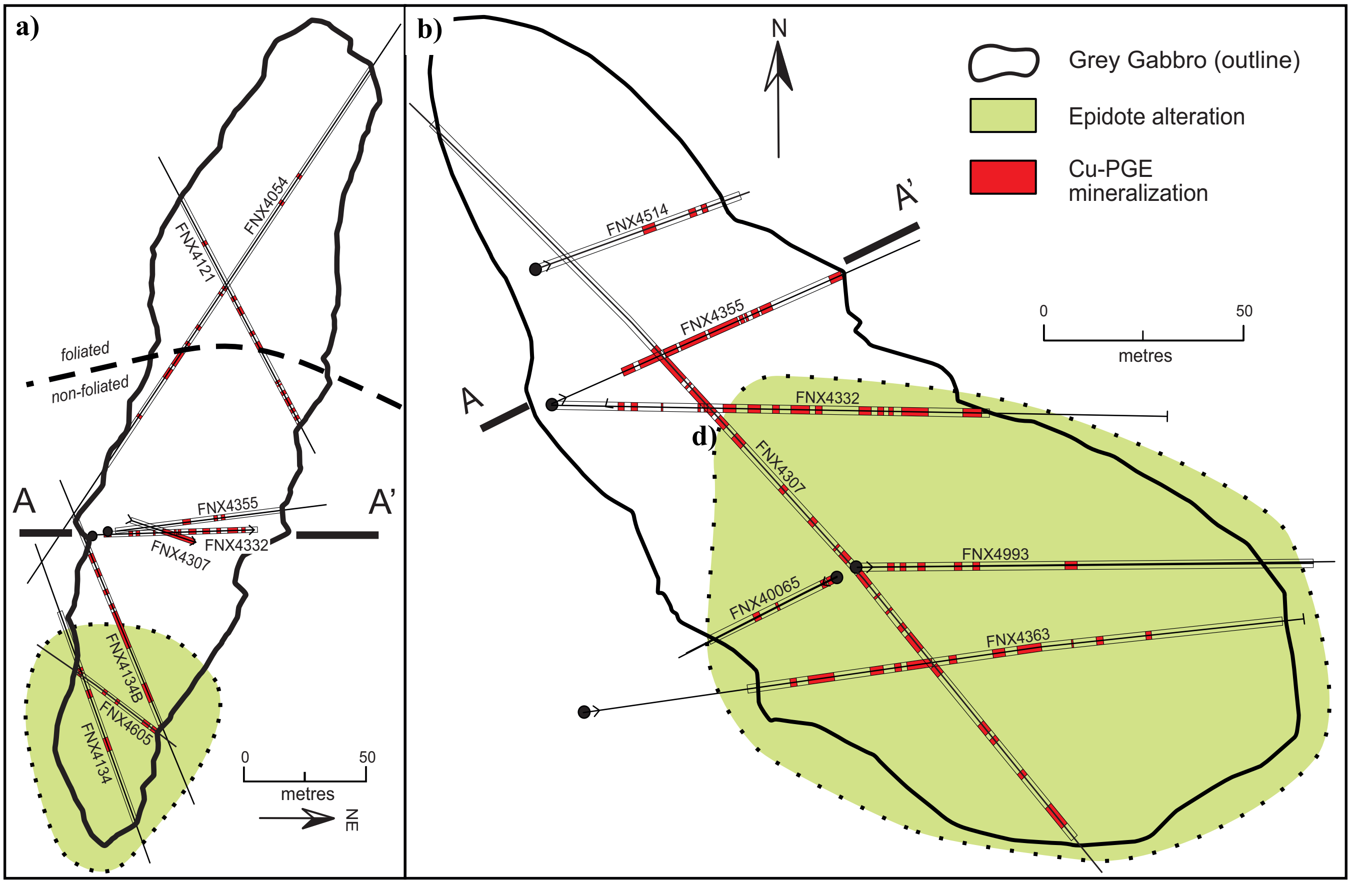

Figure 3. Remapped vertical (facing northwest) and plan view of the Podolsky Grey Gabbro fragment depicting the relationship of epidote alteration and foliation in relation to the sharp-walled Cu-(Ni)-PGE mineralization trend. Note where A and A' are in relation to the vertical and plan view maps.

ciated with the sharp-walled veins and compare it to the other known alteration present in the footwall environment of the SIC (e.g. Tuba et al., 2014 and references therein). The characterization and chemical fingerprinting of alteration-specific mineralization could provide criteria for targeting mineralization in other footwall environments.

METHODOLOGY

Mapping of the Grey Gabbro

The nature and origin of the GG unit had not previously been addressed, thus its genetic relationship to mineralization was not considered. For example, whether the GG unit was a passive host or active participant to mineralization has not been considered before this study. In order to answer this outstanding problem, the GG was studied to address two possible hypotheses: 1) The GG represented an 1850 Ma impact-generated melt compositionally related to the SIC or another source (i.e. mantle input); or 2) the GG represents a fragment of the pre-existing target area. At the time of this study, the provenance of GG was not known. To further our understanding of the unit, a comprehensive suite of 12 drillholes, which penetrated the GG unit horizontally and vertically, were re-logged using archived photos provided by KGHM International Ltd. and a geological map was produced (Fig. 3a,b). In order to assess the homogeneity of the GG unit, it was logged in 1.5 m intervals based on lithology, grain size, and texture in addition to the presence of alteration, foliation, and mineralization. The intensity of mineralization and alteration were also assessed based on the relative abundances of present phases present (see MacInnis et al., 2014). Information from several drill cores that penetrated the GG unit combined with underground visits were used to verify the maps that been produced from the photo library.

Sampling of Whole-Rock Materials and Geochemical Analysis

Seventy samples of the GG unit and its contained mineralization were collected from both underground workings and archived drill core; these samples provided the basis for petrological studies, including complete major and trace element chemistry, with a subset used for stable (O, S) and radiogenic (Sr) isotopic analysis (see below). The sample suite consisted of 19 least altered GG samples, 30 altered samples of GG, and 21 mineralized samples. The underground samples were collected between the 1700 and 2450 working levels of the deposit and included multiple transects leading up to sharp-walled chalcopyrite veins that were collected by using a diamond air saw. Full details of the sample locations and analytical techniques along with the geochemical data are presented in MacInnis et al. (2014).

Isotopic Analysis (O, Sr, S) and Geochronology (U-Pb and Ar-Ar dating)

A total of 20 samples, including nineteen whole-rock samples of the GG and one actinolite separate (see Fig. 2g), were analyzed for $\delta^{18}O$ at the Queen's University Facility for Isotopic Analysis, Kingston, Ontario. The same actinolite separate, 2 samples of least altered GG, a sample of the Joe Lake gabbro, which is an inferred-age equivalent to the GG (see below)), and, for comparison with SIC compositions, 9 North Range offset dyke samples and 1 South Range grey gabbro (Segway), were analysed for $^{87}Sr/^{86}Sr$ isotopes at the Carleton University Isotope, Geochemistry and Geochronology Research Centre, Ottawa, Ontario. A comprehensive suite of 15 chalcopyrite samples collected from massive chalcopyrite sharp-walled veins in the GG, which included 3 detailed transects from 4 levels of the mine, were analysed for sulphur isotopes ($\delta^{34}S$) at the G.G. Hatch Isotope Laboratories, Ottawa, Ontario. Methods and results for O, Sr, and S isotopic analyses are provided in MacInnis et al. (2014) and MacInnis (M.Sc. thesis, in prep.).

A sample of least altered, medium-grained GG with "salt-and-pepper" texture from the 1700 level of the Podolsky mine was selected for U-Pb zircon geochronology and was processed using conventional methods at the Geological Survey of Canada (sample 11AV-74; lab number z10633). The zircon separates, along with the host rock, were first characterized petrographically, which was followed by scanning electron microscopy (SEM) with backscattered electron (BSE) and catholuminescence (CL) imaging to fully characterize the unusual habit of the zircon (see the more detailed discussion below). The zircon grains were then dated using both isotope dilution-thermal ionization mass spectrometry (ID-TIMS; Mattinson, 2005) and the sensitive high-resolution ion microprobe (SHRIMP; Stern, 1997; Stern and Amelin, 2003). The same sample of actinolite used for O and Sr isotopic analyses, which was collected along the contact of the GG and a massive sulphide vein (see Fig. 2c,f), was selected for Ar-Ar dating. This vein sample was processed using standard methods (i.e. crushing, sieving, heavy liquids, hand picking) to generate a high-purity separate (Fig. 2g), which was subsequently irradiated and analysed at the Geological Survey of Canada; full details and results can be found in MacInnis et al. (2014).

RESULTS AND SUMMARY

Map of the Grey Gabbro Unit

Figure 3 shows a plan (1925 level) and sectional map for the GG unit and highlights the distribution of epidote alteration and mineralization, the latter represented by sharp-walled sulphide veins. The epidote alteration is confined to a portion of the GG and, based on mapping, does not appear to have any significant spatial association with the density of the sulphide mineralization, as might have been expected given the association of epidote with some mineralization in Sudbury area (e.g. Fraser deposit; Farrow and Watkinson, 1996). In addition, a weak foliation in the GG unit was observed at its northern end. This feature is also seen microscopically as an alignment of light and dark domains (a mixture of pyroxene, amphibole, and biotite). Another feature of interest was small leucocratic pegmatite bodies (≤1–2 m^2) that occur rarely in the GG; however, these were too small and rare to portray on this map and, in addition, did not appear to have any obvious spatial distribution within the GG.

Petrology of the Grey Gabbro

The least altered GG is in general a medium- to fine-grained, homogeneous unit, with a "salt-and-pepper" texture that is somewhat analogous to ophitic textured gabbro with felsic and mafic domains (Fig. 2a,b). Rare occurrences of possible chilled margins were noted in logging the GG, which was subsequently confirmed by company geologists based on their underground observations. Detailed petrographic studies integrated with imaging and chemical analyses using an SEM coupled to an energy dispersive system (EDS) indicate that the GG records a complex, multi-stage history involving initial crystallization and deuteric alteration, a shock metamorphic event, a thermal overprint, and finally a hydrothermal alteration event, as shown in representative petrographic images in Figure 4 and summarized as follows: 1) Domains of what is inferred to have been originally single grains of magmatic plagioclase now consist of sub-domains of granoblastic-textured plagioclase of 10–50 μm and An_{50} composition (Fig. 4a,c,d). This feature is considered to reflect dynamic recrystallization due to thermal heat from the melt sheet. 2) Plagioclase is altered along internal grain boundaries and interiors to a quartz-An_{20} plagioclase-epidote assemblage (Fig. 4d) and also to sericite, due to later fluid-mediated alteration related to the sulphide veins. In rare cases, the plagioclase occurs as patches of a ternary feldspar-like orthoclase phase. Interstitial to the grains are mafic clots consisting of mixed silicates (i.e. pyroxene, amphibole, biotite, Fe-Ti oxides, actinolite; Fig. 4e,f), which have a bulk composition equating to stoichiometric augitic pyroxene. These

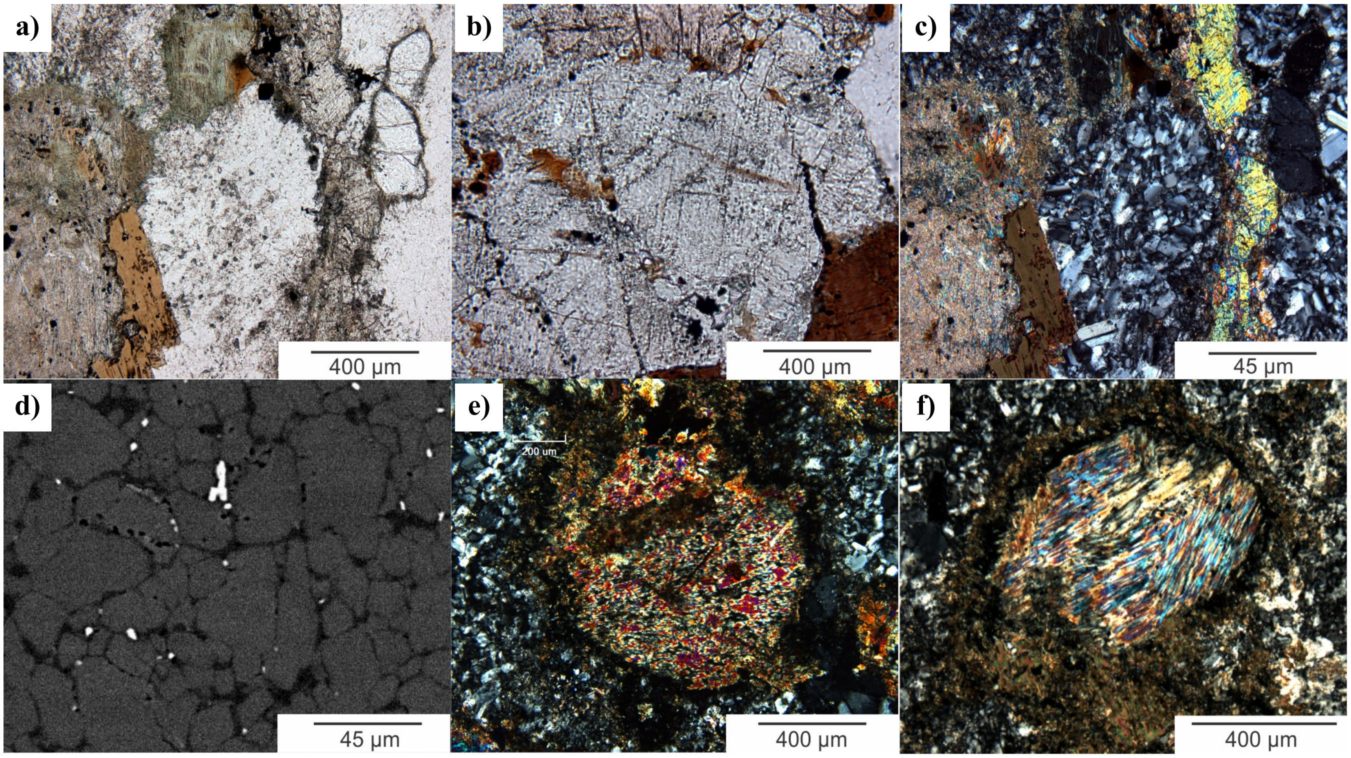

Figure 4. Photomicrographs of Grey Gabbro that highlight the two main domains of primary clinopyroxene and plagioclase and also examples of alteration. **a)** Plagioclase grain (in plane polarized light) with a subhedral outline that appears to be largely (?) unaltered. Note the euhedral apatite grains to the right, and biotite and altered pyroxene grains to the left. **b)** Clinopyroxene grain (in plane polarized light) that has a subhedral outline and a fresh interior; **c)** Same plagioclase grains seen in image (a) that in cross-polarized light displays a granoblastic texture due to thermally induced recrystallization. **d)** Backscatter electron image of the granoblastic-textured plagioclase of An_{50} composition. The bright phases are epidote and the dark phases that are intergranular to plagioclase are quartz and An_{20} plagioclase. **e, f)** Examples (in cross polarized light) of clinopyroxene partially to completely pseudomorphed by actinolite.

clots likely represent the combined effects of shock-related modification to the primary magmatic augitic pyroxene and later alteration due to fluids. 3) Zircon with planar deformation features (PDFs) and overgrowths of neomorphic zircon (se discussion below). The latter features in the zircons are considered to be related to the impact event. 4) Variable development of sericite, carbonate, and epidote with some sulphides disseminated in the GG as a result of fluid infiltration during sulphide vein formation. Proximal to sharp-walled veins, the GG is enriched in hydrothermal minerals (e.g. sericite, chlorite, quartz, actinolite, calcite, epidote, magnetite) along fractures and within dissolution features; the most intense development occurs <10 cm from the sulphide veins (Fig. 2d).

The volumetrically small pegmatite bodies, which consist of albite and quartz ± potassium feldspar, are very fresh and notably do not record petrographic evidence of the complex textures seen in the GG unit, hence a different petrogenesis is probable. Further work is required, but we tentatively suggest that they may represent partial melting of the GG due to thermal metamorphism, which would be analogous to the generation of plagiogranite found in ophiolite complexes (e.g. Grimes et al., 2013).

The major element chemistry of the GG is very uniform, which is consistent with our drill-core logging and petrographic study, and equates to a gabbro of 50 wt% SiO_2 with some chemical evidence of a cumulate component (i.e. clinopyroxene accumulation). In addition, a subalkaline character for the GG is indicated from its Zr/TiO_2 ratio. The elemental abundances and mantle-normalized profile for the trace element data show enrichment of the large ion lithophile elements (LILE), depletion of high field strength elements (HFSE: in particular strongly negative Ta-Nb anomalies), a strong fractionation of the rare earth elements (REE) with (La/Lu)N ~40, and only a slightly negative Eu anomaly; these geochemical features are consistent with derivation of the GG from a previously metasomatized subcontinental lithospheric mantle reservoir. When compared to other intrusive rocks in the Sudbury area (e.g. dyke rocks, SIC units), the GG is geochemically most similar to the 2657± 9 Ma (Bleeker et al., 2013) Joe Lake intrusion that is located just west of Podolsky (Fig. 1). In broader terms, the trace-element chemistry and extended spider plots compare most favourably to those of ocean island basalts (OIB; Sun and McDonough, 1989).

Petrology of Altered Grey Gabbro

Adjacent to sharp-walled sulphide veins, the GG unit records two features that reflect reaction with a fluid. The first feature, seen immediately against the sulphide veins, is the presence of a thin layer of mono-mineralic actinolite fibres that are <1 to 2 cm in width and are oriented perpendicular to the wall rock GG (Fig. 2d-f). The second feature is intense alteration haloes of actinolite-epidote-quartz-sulphide-magnetite-chalcopyrite. These alteration haloes are <1to 2 cm wide and are bordered by a zone of variably altered GG that gives way to least altered GG over 10 to 30 cm. The most notable petrographic feature of this alteration as observed in thin section is the presence of a network of connected pores that are commonly lined with epidote-actinolite-magnetite±chalcopyrite; these features are spatially coincident with the sericitic alteration of plagioclase near rare carbonate veins. We also note that quartz nearest the sulphide veins is intergrown with epidote and contains abundant hypersaline fluid inclusions with multi-solid phases that are petrographically similar to those observed in PGE-rich, low-sulphide footwall systems of the Sudbury Structure (e.g. Farrow et al., 1994; Molnár et al., 2001; Péntek et al., 2011; Tuba et al., 2014).

Geochemical analyses of samples collected across these alteration zones did not reveal appreciable chemical or mass change except close to the sharp-walled sulphide veins where the most altered samples show a mass gain relative to least altered samples and minor development of Eu anomalies due to alteration of plagioclase. Absolute changes in metal abundances occurred over only short distances from the veins (<20–30 cm), in particular gains of Cu, Ni, Au, Sn, Pd, Pt, Ag, and Zn. Interestingly, Cu is singularly enriched furthest from the veins without accompanying metal enrichment. In addition, sulphur, ferric iron, and loss on ignition reflected some mass gains relative to all other elements.

Stable and Radiogenic Isotopes

Oxygen isotopes were measured on four samples of least altered samples of GG and for traverses away from the veins into the GG; there was no apparent spatial correlation between $\delta^{18}O$ values of the GG unit and the sharp-walled chalcopyrite veins. The $\delta^{18}O$ values for the least altered GG of 6.7 to 8.1‰ (average = 7.3‰) compare to values of 6.5 ± 0.5‰ for samples from traverses adjacent the sharp-walled veins (see MacInnis et al. (2014) for data and details of samples). The $\delta^{18}O$ data indicate that there was no modification of the $\delta^{18}O$ signature of the GG due to vein-related fluid infiltration and is consistent, which is in agreement with the geochemical data discussed previously. An actinolite separate collected from immediately against the sulphide vein had a $\delta^{18}O$ value of 5‰, which equates to a $\delta^{18}O_{H_2O}$ value between 6.1 and 6.9‰ at 400 to 600°C (Zheng, 1993) and is consistent with a fluid of unknown origin equilibrating with the GG unit and generating the actinolite under a low fluid:rock ratio and, hence, inheriting the $\delta^{18}O$ value of the GG unit.

Table 1. Sr isotope whole-rock data for mafic rocks in the Sudbury mineral district.

Sample	$\frac{^{87}Sr}{^{86}Sr}$ i	$\frac{^{87}Rb}{^{86}Sr}$	$\frac{^{87}Sr}{^{86}Sr}$[1]	±SE[2]	Description of Lithology
[a]**Podolsky Cu-PGE deposit**					
LM-P-007	0.70183	0.1279	0.70683	0.000024	Least altered Grey Gabbro
LM-P-043G	0.70079	0.1812	0.70787	0.000008	Representative Grey Gabbro
LM-P-060	0.70209	0.0776	0.70512	0.000005	Intensely altered Grey Gabbro (actinolite separate)
[a]**Levack gneiss gabbro**					
12-AV-44	0.70167	0.0877	0.70509	0.000019	Joe Lake mafic intrusion
[b]**Offset dykes, SIC**					
13-AV-06	0.70577	0.4148	0.71681	0.000020	Hess quartz diorite, margin
13-AV-08	0.70969	0.7164	0.72876	0.000014	Ermatinger quartz diorite, core
13-AV-10	0.69999	0.7157	0.71905	0.000015	Ermatinger quartz diorite, core
13-AV-12	0.71785	0.6991	0.73645	0.000006	Ministic quartz diorite, core
13-AV-13	0.70608	0.1622	0.71040	0.000006	Parkin quartz diorite, margin
13-AV-15	0.70708	0.4763	0.71976	0.000006	Parkin quartz diorite, margin
13-AV-17	0.71042	1.0357	0.73799	0.000012	Pele quartz diorite, margin
05-AV-15	0.71038	0.3218	0.71895	0.000005	Segway grey gabbro
13-AV-04	0.70722	0.4904	0.72027	0.000052	Trill quartz diorite, core
05-AV-33	0.67327	1.1956	0.70509	0.000019	Trill quenched quartz diorite

[1]analyzed with Thermofinnigan Triton T1 thermal ionization mass spectrometer, IGGRC Carleton University
[2]Uncertainties are presented as ±2 standard errors (SE)
[a]initial Sr (i) calculated at 2700Ma, [b]initial Sr (i) calculated at 1850 Ma

Sulphur isotopic data across the sharp-walled veins (<1 m thick) are consistent with an average $\delta^{34}S$ value of 4.3 ± 0.3‰ (McInnis et al., 2014). These values are similar to those reported by other workers for the sulphide mineralization related to the SIC (e.g. Ames et al., 2010; Tuba et al., 2014), and therefore indicate a uniform isotopic reservoir for the S. This also suggests that the sulphides were deposited in the Whistle-Podolsky ore system under similar physio-chemical conditions since no variation, which would result from fractionation, is recorded. Furthermore, the data are consistent, as expected, with a dominantly crustal reservoir for the S versus a mantle source (i.e. departure from 0‰; Ohmoto and Rye, 1979).

Strontium isotopic data (i.e. $^{87}Sr/^{86}Sr$, Table 1) obtained for two samples of least altered GG indicate measured $^{87}Sr/^{86}Sr$ values of 0.70512, 0.70683, and 0.70787, which give age-corrected initial Sr isotope (Sr_i) values of 0.70079 to 0.70209 at 2700 Ma, the minimum estimated time for crystallization of the GG (see below), and Sr_i values of 0.70305 and 0.703042 at 1850 Ma, the age of the impact event and the sulphide mineralization. The Sr_i values for the GG at 2700 Ma overlaps with a single Sr_i value of 0.70167 for the geochemically similar Joe Lake gabbro (also at 2700 Ma, Table 1) and are much lower than the Sr_i values for the offset dyke component of the radiogenic SIC (6 North Range offset dykes; Table 1). The single actinolite sample analysed yielded an initial $^{87}Sr/^{86}Sr$ value of 0.70305, its low Rb content not requiring age-correcting. That the initial $^{87}Sr/^{86}Sr$ value for the actinolite is similar to the GG value at 1850 Ma suggests that the actinolite formed due to reaction of a fluid with the GG at this time and is consistent with the $^{40}Ar/^{39}Ar$ dating of the actinolite (see below).

Geochronology

$^{40}Ar/^{39}Ar$ Age Dating

The results of 10 out of 14 total fusion analyses of actinolite grains from adjacent a sharped-wall sulphide vein indicate a weighted mean age of 1850 ± 30 Ma (see MacInnis et al. (2014) for full results). This age is interpreted to record cooling of the actinolite below the argon blocking temperature, which is taken to be around 350 to 400°C in this phase (McDougall and Harrison, 1999). Importantly, the age overlaps (within error) the time of the Sudbury impact event (1849.53 ± 0.21 Ma; Davis, 2008) and indicates, therefore, that in the study area a subsequent reheating to above 350 or 400°C did not occur after 1820 Ma, although we cannot say it did not occur prior to this time and after 1850 Ma. This latter interpretation is further verified based on the results of step-wise heating of actinolite grains from the same sample, which yielded flat age spectra profiles (MacInnis et al., 2014).

Zircon Morphology and U-Pb Thermal Ionization Mass Spectrometry and Sensitive High-Resolution Ion Microprobe Dating

Zircon Morphology

Examination of the zircon hosted by the GG unit indicated two distinct morphological types which, based on their proportions in the mineral separate prepared for dating, appear to be in roughly equal proportion. One of these zircon sub-populations consists of clear, colourless, euhedral, prismatic (elongate to stubby), well faceted, and terminated crystals with few fractures and rare clear inclusions (Fig. 5a). When examined in CL (Fig. 5b), the euhedral zircon grains are strongly luminescent and exhibit sharp oscillatory and sector zoning, which are features most commonly ascribed to growth from a silicate melt (Corfu et al., 2003). This morphological type of clear zircon was analysed for U-Pb dating by isotope dilution - thermal ionization mass spectrometry (ID-TIMS).

The second zircon sub-population consists of highly fractured, anhedral, pale brown to reddish brown, cloudy fragments (Fig. 5c) that occur as cores to the overgrowths of the clear, colourless zircon, which is tentatively linked to the euhedral morphology described above. The fractured zircon has relatively poor CL response, appearing as medium to dark grey (Fig. 5d), whereas the clear overgrowths luminesce strongly (Fig. 5d). Corresponding back scatter electron (BSE) images faintly mimic the zoning in the CL images, but more clearly illustrate the presence of fractures and inclusions (Fig. 5d). The BSE images clearly show that anhedral zircon is characterized by the presence of crystallographically oriented features, including short fractures or small pits. These features have been noted in zircons elsewhere and were attributed to planar deformation features resulting from shock impact (Krogh et al,. 1984; Bohor et al, 1993; Krogh et al., 1993a, b; Pidgeon et al., 2011). Anhedral zircon, both with and without the euhedral overgrowths, was analysed for U-Pb dating by sensitive high-resolution ion microprobe (SHRIMP).

U-Pb Age Dating

Six single-grain fractions of euhedral zircon were analysed using ID-TIMS with five of the most concordant analyses (0.1–0.3%) yielding a mean $^{207}Pb/^{206}Pb$ age of 1849.9 ± 1.0 Ma; the sixth zircon analysed was more discordant (0.7%) and gave an age of 1854 Ma (Fig. 6, Table 2). The 1849.9 ± 1.0 Ma age is considered to represent the time at which these euhedral zircon grains grew, which is equate to the Sudbury impact event. Twenty-one U-Pb SHRIMP analyses were carried out on fifteen anhedral zircon grains, with a few analyses also hitting the euhedral overgrowths on these grains. These zircon analyses yielded a range of $^{207}Pb/^{206}Pb$ ages between 2606 Ma and 1706 Ma and were typically 3-10% discordant. Examination of the data in a concordia diagram (Fig. 6b) indicate that a linear array is defined with an upper intercept of ca. 2714 ± 52 Ma, which is derived by anchoring the lower intercept at 1850 Ma, the inferred time of impact and resetting of the zircons (Fig. 6b, Table 3). The upper intercept is considered the best approximation of a minimum age for the GG, whereas the lower intercept is considered to reflect a resetting event and when the PDF in the zircon formed, which equates to the time of the Sudbury impact event.

SUMMARY OF THE FINDINGS AND IMPLICATIONS FOR EXPLORATION

1. The GG unit represents a large dislodged fragment of a previously crystallized alkali gabbro rock that formed at or before ca. 2714 Ma. This unit is correlated with its petrologically equivalent unit in the North Range footwall environment, the Joe Lake Gabbro, which has a minimum age of ca. 2657 ± 9 Ma based on U-Pb dating of inferred metamorphic

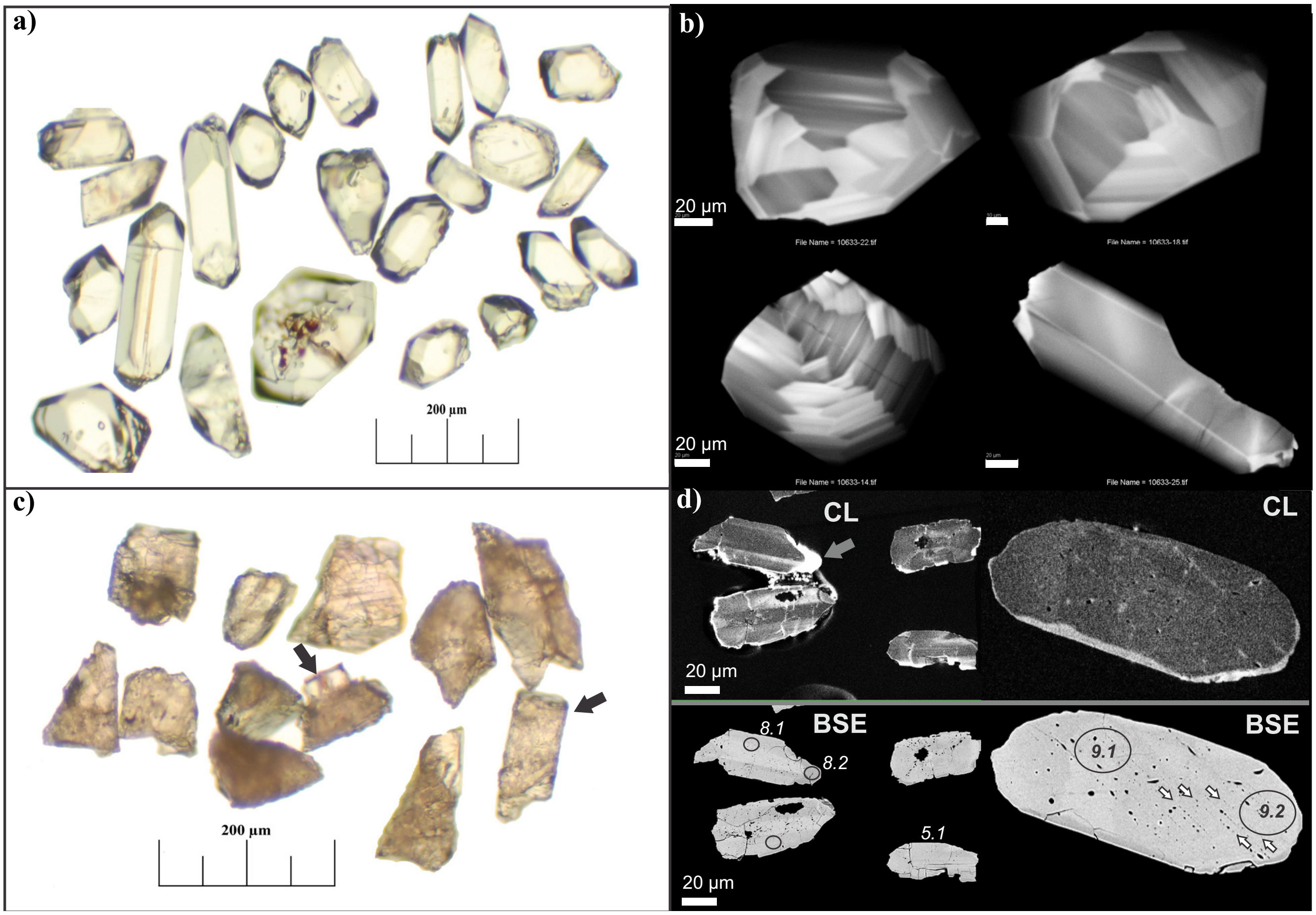

Figure 5. Photographs summarizing the various textures of zircon extracted from a sample of Grey Gabbro. **a)** Transmitted light photomicrograph of euhedral, prismatic zircon grains, after annealing for 48 h at 1000°C; photograph includes zircon grains analysed by TIMS. **b)** Cathodolumi-nescence (CL) images of euhedral, prismatic zircon. **c)** Transmitted light photomicrograph of anhedral zircon inferred to record shock metamorphic textures; some of these grains were selected for SHRIMP analysis. The arrows indicate the presence of overgrowths of euhedral zircon on the earlier, shocked zircon. **d)** Complementary CL (top) and BSE (bottom) images of shocked zircon with the grey arrow indicating an area of zircon overgrowth. Note the enhanced brightness of the euhedral zircon overgrowth relative to the anhedral shocked zircon. The crystallographically oriented features seen in the BSE (indicated by pairs of small, white arrows) are interpreted as impact-related planar deformation features. SHRIMP analysis sites are shown by black ellipses labelled with corresponding spot name shown in Table 3.

zircons (Bleeker et al., 2013). The geochemistry of the GG, and also the age and geochemically equivalent Joe Lake gabbro, indicates it was sourced from a previously metasomatised subcontinental lithospheric mantle and is unrelated to the SIC.

2. The GG is a macroscopically homogeneous unit, but detailed petrographic and SEM-EDS imaging studies indicate a complex textural history that involved extensive mineral re-equilibration. The latter feature is interpreted to reflect shock-induced metamorphism at ca. 1850 Ma due to the Sudbury impact event (e.g., zircon PDF features and overgrowths), then shortly thereafter thermal annealing related to the cooling melt sheet that overlay the site (e.g. plagioclase textures), and then superimposed hydrothermal alteration related to the emplacement of sharp-walled sulphide veins.
3. $^{40}Ar/^{39}Ar$ age-dating of actinolite found along the contact of GG and sharp-walled sulphide veins records cooling of the area below ~350–400°C at ca. 1850 Ma and, furthermore, its flat age spectra indicates the area did not subsequently experience heating above this temperature.
4. Hydrothermal alteration of the GG adjacent to the sharp-walled sulphide veins is most intense nearest the veins (i.e. ≤10–20 cm) with formation of a quartz-epidote-actinolite-magnetite-chalcopyrite zone that quickly becomes cryptic into the wall rock. Geochemically, the most distal indicator of the mineralization is elevated Cu (to 100s ppm up to 1 m away) without enrichment of other metals.
5. Isotopic analyses (Sr, O, S) indicate that the GG retains its primary isotopic signal for Sr and O despite alteration, whereas the O data for actinolite records $\delta^{18}O_{H_2O}$ values of 6.1 to 6.9‰ at 400 to

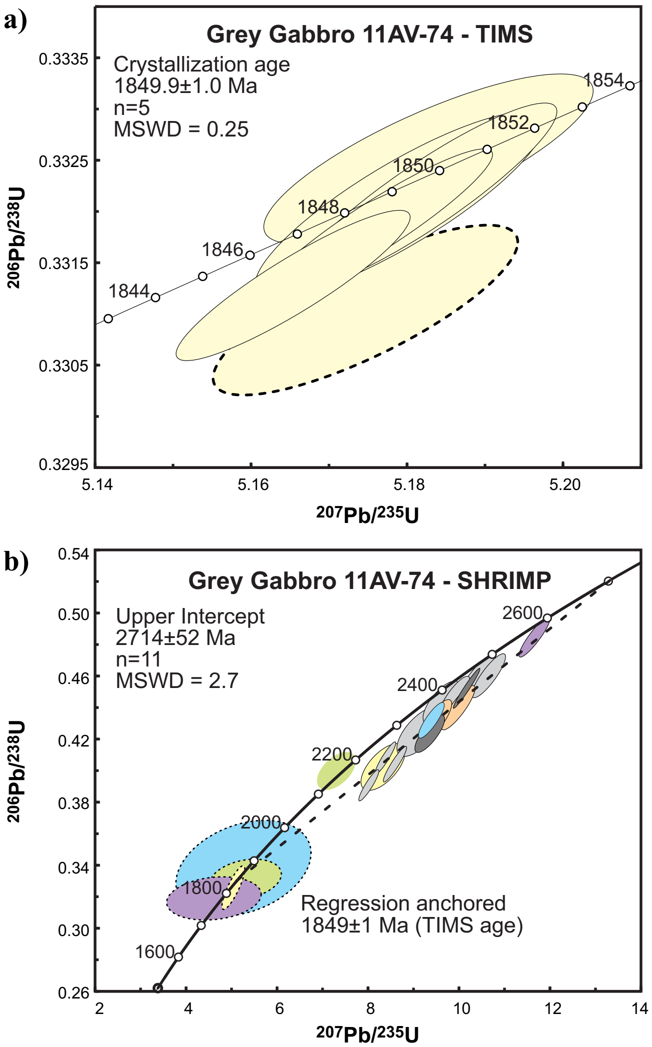

Figure 6. U-Pb concordia diagrams for zircon from the Grey Gabbro unit. a) Results for six zircon grains analysed by ID-TIMS with error ellipses plotted at 2σ. The calculated age of 1849.9 Ma excluded the most discordant sample, which is shown by the dashed ellipse. b) Results of SHRIMP analyses with error ellipses plotted at 2σ. Note the following: (1) pairs of analyses on a single grain are shown by colours other than light grey, (2) analyses of shocked zircon grains are shown by solid outlines and cluster towards 2400 Ma, (3) euhedral overgrowths are shown by dashed outlines and cluster at 1800 to 2000 Ma, and (4) the analysis excluded from regression (ellipse at 2200 Ma) is shown with no outline. Note that the regression line shown (dashed line) is anchored at 1850 Ma, the time of the impact event at Sudbury.

Table 2. U-Pb TIMS analytical data of six grain fractions of a euhedral zircon found in sample 11AV-74 (Z10633).

Fract.[1]	Description[2]	Wt. ug	U ppm	Pb[3] ppm	$^{206}Pb/^{204}Pb$[4]	Pb[5] pg	$^{208}Pb/^{206}Pb$	$^{207}Pb/^{235}U$	±1SE Abs	$^{206}Pb/^{238}U$	±1SE Abs	Corr.[7] Coeff.	$^{207}Pb/^{206}Pb$	±1SE Abs	$^{206}Pb/^{238}U$	±2SE	$^{207}Pb/^{235}U$	±2SE	$^{207}Pb/^{206}Pb$	±2SE	% Disc
Sample 11AV-74 (Z10633)																					
A16-1	Clr, Co, El, Pr, NM0	4	51	29	1781	2	0.87	5.1789	0.0075	0.33207	0.00037	0.857111505	0.11311	0.00009	1848.4	3.6	1849.1	2.5	1850.0	2.7	0.1
A16-2	Clr, Co, El, Pr, NM0	5	78	45	3977	2	0.90	5.1652	0.0061	0.33128	0.00030	0.908397397	0.11308	0.00006	1844.6	2.9	1846.9	2.0	1849.5	1.9	0.3
A16-3	Clr, Co, St, Pr, nIn, NM0	12	21	12	1190	4	0.84	5.1745	0.0080	0.33104	0.00034	0.800901953	0.11337	0.00011	1843.4	3.3	1848.4	2.6	1854.1	3.4	0.7
C16-1	Clr, Co, El, Pr, M1	6	59	35	7873	1	0.98	5.1758	0.0061	0.33186	0.00031	0.926939444	0.11311	0.00005	1847.4	3.0	1848.6	2.0	1850.0	1.7	0.2
C16-2	Clr, Co, El, Pr, M1	6	33	19	3776	0	0.92	5.1821	0.0069	0.33216	0.00037	0.908311575	0.11315	0.00006	1848.8	3.5	1849.7	2.3	1850.6	2.1	0.1
C16-3	Clr, Co, El, Pr, M1	4	42	24	975	4	0.93	5.1826	0.0086	0.33252	0.00034	0.800641518	0.11304	0.00012	1850.6	3.3	1849.8	2.8	1848.8	3.7	-0.1

[1]All zircon fractions are composed of single grains and were chemically abraded using a modified procedure from Mattinson (2005); all fractions composed of single grains
[2]Zircon descriptions: Co=colourless, Clr=clear, El=elongate, Eu=euhedral, nIn=numerous inclusions, Pr=prismatic, St=stubby prism, NM0=non-magnetic @1.8A 0oSS, M1=magnetic @ 1.8A 1oSS.
[3]Radiogenic Pb
[4]Measured ratio, corrected for spike and fractionation
[5]Total common Pb in analysis corrected for fractionation and spike
[6]Corrected for blank Pb and U and common Pb, errors quoted are 1 sigma absolute; procedural blank values for this study are 0.1 pg U and 1 pg Pb
Pb blank isotopic composition is based on the analysis of procedural blanks; corrections for common Pb were made using Stacey and Kramers (1975) compositions
[7]Correlation Coefficient
[8]Corrected for blank and common Pb, errors quoted are 2σ in Ma
The error on the calibration of the GSC ^{205}Pb-^{233}U-^{235}U spike utilized in this study is 0.22% (2s)

Table 3. U-Pb SHRIMP analytical data for zircon from sample 11AV-74 (Z10633).

Spot name	U (ppm)	Th (ppm)	Th/U	Yb (ppm)	Hf (ppm)	$^{204}Pb/^{206}Pb$	% ±	$^{206}Pb^*$ (ppm)	$f(206)^{204}$ %	$^{208*}Pb/^{206*}Pb$	% ±	$^{207*}Pb/^{235}U$	% ±	$^{206*}Pb/^{238}U$	% ±	Corr Coeff	$^{207*}Pb/^{206*}Pb$	% ±	$^{206*}Pb/^{238}U$	±	$^{207*}Pb/^{206*}Pb$	±	Disc. %
10633-8.2	11	20	1.94	61	7870	3.2E-3	20	3	5.587	0.547	4.2	4.60	9.3	0.319	1.75	0.188	0.1046	9.2	1784	27	1707	169	-5.2
10633-36.2	29	51	1.85	79	9640	7.9E-5	46	8	0.137	0.575	2.9	5.03	2.1	0.325	1.74	0.845	0.1121	1.1	1816	28	1834	20	1.1
10633-1.2	12	20	1.74	64	7091	3.4E-3	20	3	5.821	0.476	3.8	5.25	11.6	0.338	3.67	0.315	0.1128	11.0	1876	60	1845	200	-1.9
10633-2.2	19	34	1.86	73	7716	2.4E-3	20	5	4.154	0.552	3.0	5.29	6.1	0.331	1.56	0.254	0.1160	5.9	1843	25	1896	107	3.2
10633-2.1	89	122	1.42	121	9867	8.9E-4	20	30	1.536	0.418	2.4	7.31	2.4	0.399	1.23	0.518	0.1326	2.0	2167	23	2133	36	-1.8
10633-7.1	126	242	1.98	182	9100	3.0E-5	85	44	0.052	0.574	1.1	8.39	1.1	0.408	1.03	0.927	0.1491	0.4	2206	19	2335	7	6.6
10633-15.1	81	87	1.10	67	9579	-2.7E-5	37	27	-0.047	0.330	1.8	8.03	1.1	0.390	1.04	0.915	0.1491	0.5	2125	19	2336	8	10.6
10633-36.1	38	55	1.52	81	7516	3.1E-4	64	13	0.531	0.429	2.3	8.34	2.4	0.402	1.50	0.632	0.1504	1.8	2179	28	2351	32	8.6
10633-19.1	111	226	2.10	204	6823	3.6E-5	41	38	0.063	0.623	1.1	8.61	1.2	0.404	1.14	0.930	0.1545	0.4	2187	21	2396	8	10.3
10633-6.1	108	197	1.90	181	10083	2.8E-4	62	39	0.490	0.546	2.2	9.15	2.3	0.425	1.51	0.668	0.1562	1.7	2281	29	2415	28	6.6
10633-10.1	161	404	2.58	306	7629	5.4E-5	234	61	0.094	0.746	1.4	9.63	1.7	0.443	1.24	0.718	0.1576	1.2	2364	25	2430	20	3.2
10633-1.1	69	146	2.19	153	6941	1.7E-4	33	26	0.298	0.643	1.3	9.40	1.2	0.432	1.07	0.857	0.1579	0.6	2313	21	2434	11	5.9
10633-23.2	90	189	2.16	191	7685	1.8E-4	34	34	0.310	0.601	1.9	9.49	1.6	0.432	1.27	0.803	0.1594	0.9	2313	25	2449	16	6.6
10633-9.1	173	202	1.21	185	10034	2.6E-4	28	63	0.448	0.336	2.1	9.37	1.4	0.423	1.14	0.789	0.1605	0.9	2275	22	2461	15	8.9
10633-21.1	139	257	1.91	211	8744	6.8E-5	65	51	0.117	0.548	1.0	9.49	1.1	0.428	1.03	0.897	0.1608	0.5	2298	20	2464	9	8.0
10633-11.1	105	207	2.04	205	8034	8.7E-5	21	40	0.150	0.572	1.9	9.92	1.4	0.447	1.17	0.842	0.1610	0.7	2381	23	2466	13	4.1
10633-9.2	232	212	0.95	149	11253	2.2E-5	41	90	0.038	0.275	1.1	10.19	1.2	0.452	1.14	0.971	0.1635	0.3	2405	23	2492	5	4.2
10633-23.1	132	249	1.95	221	8729	5.3E-5	50	50	0.092	0.521	1.9	10.00	1.5	0.440	1.31	0.865	0.1650	0.8	2350	26	2507	13	7.5
10633-4.1	64	106	1.71	108	8233	4.8E-5	71	25	0.083	0.474	2.6	10.44	1.6	0.458	1.28	0.793	0.1653	1.0	2432	26	2511	17	3.8
10633-5.1	85	167	2.02	184	8385	-1.1E-5	38	34	-0.019	0.577	1.9	10.67	1.4	0.460	1.24	0.861	0.1683	0.7	2439	25	2541	12	4.8
10633-8.1	221	571	2.67	376	7531	7.7E-5	39	92	0.133	0.757	1.1	11.70	1.2	0.485	1.08	0.903	0.1750	0.5	2548	23	2606	9	2.7

Spot name follows the convention x-y.z; where x = sample number, y = grain number and z = spot number

$f(206)^{204}$ refers to mole percent of total ^{206}Pb that is due to common Pb, calculated using the ^{204}Pb-method; common Pb composition used is the surface blank (4/6: 0.05770; 7/6: 0.89500; 8/6: 2.13840)

* refers to radiogenic Pb (corrected for common Pb)

Errors are reported at 1σ uncertainty level unless otherwise noted

Analytical details:

IP665: 25 μm spot; 5 or 6 scans; ~9nA O- primary beam intensity, U-Pb calibration error 1.0% (included)

No mass fractionation correction applied

600°C, which suggests isotopic equilibration with the GFG unit at low fluid:rock interaction. The S isotopic data for the sharped-wall vein sulphides, with average $\delta^{34}S$ value of 4.3‰, is consistent with a single homogeneous crustal reservoir, which was likely sourced from the melt sheet.

In summary, this study has shown that the GG is part of the pre-impact history at 1850 Ma and although there is an intense hydrothermal alteration adjacent to the sharp-walled sulphide veins, its extent is limited to 10s cm and thus does not provide a significant vector for exploration.

FORTHCOMING PRODUCTS

A petrological and geochronological study of the grey gabbro unit of the Podolsky Cu-Ni-PGE deposit, Sudbury, Ontario: A 2.6 Ga Gabbro Hosting 1.85 Ga impact-related mineralization. Authors: Linette M. MacInnis, Daniel J. Kontak, Doreen E. Ames, and Nicole Rayner, January, 2015, CJES.

The chemical fingerprint of alteration marginal to a sharp-walled Cu(-Ni)-PGE vein setting: Podolsky deposit, Sudbury, Ontario. Authors: Linette M. MacInnis, Daniel J. Kontak, Doreen E. Ames, and Nancy Joyce, January 2015, SEG.

ACKNOWLEDGEMENTS

The authors would like to thank KGHM International Ltd.'s Podolsky 2012-2013 team for their guidance, access, feedback, coordination, and insight with their computer programs, facilities, and logistics. This work was initiated and funded by the Targeted Geoscience Initiative 4 (TGI-4) program of the Geological Survey of Canada (GSC) within the Ni-Cu-PGE–Cr project including support to the second author (L.M. MacInnis) under the Research Affiliate Program 2012-2014 of Natural Resources of Canada.

REFERENCES

Ames, D.E. and Farrow, C.E.G., 2007. Metallogeny of the Sudbury mining camp, Ontario; Geological Association of Canada, Mineral Deposits Division, Special Publication 5, p. 329–350.

Ames, D.E., Golightly, J.P. and Zierenberg, R.A., 2010. Trace element and sulfur isotope composition of Sudbury Ni-Cu-PGE ores in diverse settings, *In:* Extended Abstracts;. Society of Economic Geologists (SEG), 2010 Keystone conference, Keystone, Colorado, October 2–5, 2010, 4 p. (DVD).

Bleeker, W., Kamo, S., and Ames, D., 2013. New field observations and U-Pb age data for footwall (Target) rocks at Sudbury: Towards a detailed cross-section through the Sudbury Structure, *In:* Lunar and Planetary Institute Abstract Collection; Lunar and Planetary Institute Conference, Large Meteorite Impacts and Planetary Evolution V, Sudbury, Ontario, August 5 to 8, 3112.pdf.

Bohor, B.F., Betterton, W.J., and Krogh, T.E., 1993. Impact-shocked zircons: discovery of shock-induced textures reflecting increasing degrees of shock metamorphism; Earth and Planetary Science Letters, v. 119, p. 419–424.

Carter, W.M., Watkinson, D.H., Ames, D.E., and Jones, P.C., 2009. Quartz diorite magmas and Cu-(Ni)-PGE mineralization, Podolsky deposit, Whistle offset structures, Sudbury, Ontario; Geological Survey of Canada, Open File 6134, 58 p., 1 CD-ROM. doi:10.4095/247514

Corfu, F., Hanchar, J.M., Hoskin, P.W.O., and Kinny, P., 2003. Atlas of zircon textures; Reviews in Mineralogy and Geochemistry, v. 53, p. 469–500.

Davis, D., 2008. Sub-million-year age resolution of Precambrian igneous events by thermal extraction-thermal ionization mass spectrometer Pb dating of zircon: Application to crystallization of the Sudbury impact melt sheet; Geology, v. 36, p. 383–386.

Farrow, C.E.G., Watkinson, D.J., and Jones, P.C., 1994. Fluid inclusion in sulfides from North and South Range Cu-Ni-PGE deposit, Sudbury Structure, Ontario; Economic Geology, v. 89, p. 647–655.

Farrow, C.E.G. and Watkinson, D.H., 1996. Geochemical evolution of the epidote zone, Fraser Mine, Sudbury, Ontario: NI-Cu-PGE remobilization by saline fluids; Exploration and Mining Geology, v. 5, p. 17–31.

Farrow, C.E.G., Everest, J.O., King, D.M., and Jolette, C., 2005. Sudbury Cu-(Ni)-PGE systems: Refining their classification using McCreedy West Mine and Podolsky Project Case Studies, *In:* Exploration for Deposits of Platinum-Group Elements, (ed.) J.E. Mungall; Mineralogical Association of Canada, Short Course Series, v. 35, p. 163–180.

Grimes, C.B., Ushikubo, T., Kozdon, R., and Valley, J., 2013. Perspectives on the origin of plagiogranite in ophiolites from oxygen isotopes in zircon; Lithos, v. 179, p. 48–66.

Krogh, T.E., Davis, D.W., and Corfu, F., 1984. Precise U-Pb zircon and baddeleyite ages for the Sudbury area, *In:* Geology and Ore Deposits of the Sudbury Structure, (ed.) E.G. Pye, A.J. Naldrett, and P.E. Giblin; Ontario Geological Survey, Special Volume 1, p. 431–446.

Krogh, T.E., Kamo, S.L., and Bohor, B.F., 1993a. Fingerprinting the K/T impact site and determining the time of impact by U-Pb dating of single shocked zircons from distal ejecta; Earth and Planetary Science Letters, v. 119, p. 425–429.

Krogh, T.E., Kamo, S.L., Sharpton, V.L., Marin, L.E., and Hildebrand, A.R., 1993b. U-Pb ages of single shocked zircons linking distal ejecta to the Chicxulub crater; Nature, v. 366, p. 731–734.

Lightfoot, P.C., Keays, R.R., Morrison, G.C., Bite, A., and Farrell, K.P., 1997. Geochemical relationships in the Sudbury Igneous Complex: Origin of the Main Mass and Offset Dikes; Economic Geology, v. 92, p. 289–307.

MacInnis, L.M., Kontak, D.J., Ames, D.E., and Joyce, N.L., 2014. Alteration proximal to the sharp-walled Cu-(Ni)-PGE vein footwall mineralization of the Podolsky deposit; Geological Survey of Canada, Open File 7666, 19 p. doi:10.4095/295482

Mattinson, J.M., 2005. Zircon U-Pb chemical abrasion ("CA-TIMS") method: combined annealing and multi-step partial dissolution analysis for improved precision and accuracy of zircon ages; Chemical Geology, v. 22, p. 47–66.

McDougall, I. and Harrison, T.M., 1999. Geochronology and Thermochronology by the $^{40}Ar/^{39}Ar$ Method; Oxford University Press, New York, 269 p.

Molnár, F., Watkinson, D.H., and Jones, P.C., 2001. Multiple hydrothermal processes in footwall units of the North Range, Sudbury Igneous Complex, Canada, and Implications for the genesis of vein-type Cu-Ni-PGE deposits; Economic Geology, v. 96, p. 1645–1670.

Ohmoto, H. and Rye, R.O., 1979. Isotopes of sulphur and carbon, *In:* Geochemistry of Hydrothermal Ore Deposits, (ed.) H.L. Barnes; J. Wiley & Sons, New York, p. 509–567.

Péntek, A., Molnár, F., Watkinson, D.H., Jones, P.C., and Mogessie, A., 2011. Partial melting and melt segregation in footwall units within the contact aureole of the Sudbury Igneous Complex (North and East Ranges, Sudbury Structure), with implications for their relationship to footwall Cu-Ni-PGE mineralization; International Geology Review, v. 53, p. 291–325.

Pidgeon, R.T., Nemchin, A.A., and Kamo, S.L., 2011. Comparison of structures in zircons from lunar and terrestrial impactites; Canadian Journal of Earth Sciences, v. 48, p. 107–116.

Stacey, J.S. and Kramers, J.D., 1975. Approximation of terrestrial lead isotope evolution by a 2-stage model; Earth and Planetary Science Letters, v. 26, p. 207–221.

Stern, R.A., 1997. The GSC sensitive high-resolution ion microprobe (SHRIMP): analytical techniques of zircon U-Th-Pb age determinations and performance evaluation, in Radiogenic Age and Isotopic Studies, Report 10; Geological Survey of Canada, Current Research 1997-F, p. 1–31.

Stern, R.A. and Amelin, Y., 2003. Assessment of errors in SIMS zircon U-Pb geochronology using a natural zircon standard and NIST SRM 610 glass; Chemical Geology, v. 197, p. 111–146.

Sun, S.-S. and McDonough, F., 1989. Chemical and isotopic systematic of oceanic basalts; implications for mantle composition and processes, *In:* Magmatism in the ocean basins; Geological Society, Special Publication, v. 42, p. 312–345.

Tuba, G., Molnár, F., Ames, D.E., Péntek, A., Watkinson, D.H., and Jones, P.C., 2014. Multi-stage hydrothermal processes involved in “low-sulfide” Cu(-Ni)-PGE mineralization in the footwall of the Sudbury Igneous Complex (Canada): Amy Lake PGE zone, East Range; Mineralium Deposita, v. 49, p. 7–47.

Zheng, Y.-F., 1993. Calculation of oxygen isotope fractionation in hydroxyl-bearing silicates; Earth and Planetary Science Letters, v. 120, p. 247–263.